



# Copper-containing catalysts for solvent-free selective oxidation of benzyl alcohol

Yolanda Pérez, Ruth Ballesteros, Mariano Fajardo, Isabel Sierra, Isabel del Hierro\*

Departamento de Química Inorgánica y Analítica (E.S.C.E.T.), Universidad Rey Juan Carlos, 28933 Móstoles, Madrid, Spain

## ARTICLE INFO

### Article history:

Received 26 April 2011

Received in revised form 4 October 2011

Accepted 7 October 2011

Available online 17 October 2011

### Keywords:

Selective oxidation

Solvent-free

TBHP and H<sub>2</sub>O<sub>2</sub>

Copper-containing catalysts

MCM-41

## ABSTRACT

In this paper two different methods for the preparation of copper-containing catalysts have been described. Copper (II) ethylacetoacetate or copper (II) nitrate metallic precursors have been immobilized onto previously organofunctionalized MCM-41 material with N<sup>4</sup>-(3-(triethoxysilyl)propyl)pyrimidine-2,4,6-triamine (DAPyPTS) compound. The amino hybrid materials have been prepared by using both post-synthesis and co-condensation methods. In addition, the immobilization has been performed using organic and aqueous media. The catalysts have been characterized using X-ray diffraction (XRD), N<sub>2</sub> adsorption–desorption, inductively coupled plasma-atomic emission spectroscopy (ICP-AES), scanning electron microscope (SEM) with energy-dispersive X-ray (EDX), elemental analysis, <sup>1</sup>H, <sup>13</sup>C and <sup>28</sup>Si MAS NMR, FT-IR and DRUV–vis spectroscopy. Copper-containing catalysts have been tested in the benzyl alcohol oxidation with TBHP and H<sub>2</sub>O<sub>2</sub> as oxidants and under solventless conditions. High selective (97%) to benzaldehyde was achieved using TBHP as oxidant and copper (II) ethylacetoacetate immobilized onto organofunctionalized MCM-41 as catalyst under solventless conditions.

© 2011 Elsevier B.V. All rights reserved.

## 1. Introduction

The oxidation of alcohols into aldehydes and ketones is a significant transformation in organic chemistry with recognized industrial importance. Selective oxidation of benzyl alcohol to benzaldehyde is a practically important reaction for the production of chlorine-free benzaldehyde required in the perfumery and pharmaceutical industries [1]. Benzaldehyde, has also been employed in the synthesis of cyclic acetals, widely used for flavours, fragrances, nutritious additives and solvents [2]. Homogeneous copper complexes have been extensively studied for the oxidation of alcohols to aldehydes and ketones [3]. Although homogeneous catalysts exhibit excellent activity and selectivity, technical problems as the difficulty in product separation have slowed their industrial applications. On this way, the studies on the heterogeneous catalytic activities of single copper active sites are challenging.

Among the newer heterogeneous oxidation catalysts, copper-containing porous materials present attractive interest. Xavier et al. [4] synthesized Cu(II) complexes of dimethylglyoxime (dmgH) and N,N'-ethylenebis(7-methylsalicylideneamine) encapsulated in Y zeolite. Employing H<sub>2</sub>O<sub>2</sub> as oxidant for oxidation of benzyl alcohol in benzene, the conversion obtained were 52.6% with YCu(dmgh)<sub>2</sub> sample. Kato et al. [5] tested microporous dinuclear copper (II) trans-1,4-cyclohexanedicarboxylate in the catalytic oxidation of benzyl alcohol. H<sub>2</sub>O<sub>2</sub> as oxidant and acetonitrile as solvent were

employed to obtain 25.8% of benzyl alcohol conversion and a TON value of 12.

Others materials have been used in the oxidation of benzyl alcohol using TBHP as oxidant such as layered double hydroxides (LDH) containing different transition metals [6]. Copper (II) anchored on L-valine bound poly(styrene–divinylbenzene) co-polymer [7] has also been used achieving 72% of benzyl alcohol conversion, 93.8% of selectivity towards benzaldehyde.

Oxidation of benzyl alcohol is being investigated to perform under solventless conditions and using molecular oxygen or hydrogen peroxide as oxidants. This represents a much cheaper, safer and more environmentally benign oxidation protocol. Choudhary et al. [8] have tested the performance of copper containing hydrotalcite-like solid catalysts in the solvent-free oxidation of benzyl alcohol using molecular oxygen as oxidant. Conversion and selectivity obtained were 41% and 70.8%, respectively. Recently, Bansal et al. [9] have synthesized tetraazamacrocyclic complexes of Cu(II) and Ni(II) encapsulated in zeolite-Y for oxidation of benzyl alcohol using H<sub>2</sub>O<sub>2</sub>. The best catalytic result was achieved using 7,16-diacetyl[Cu{Me<sub>4</sub>(Bzo)<sub>2</sub>[14]tetraeneN<sub>4</sub>}-NaY as catalyst showing 29.9% conversion of benzyl alcohol in 6 h and selectivity value for benzaldehyde of 96.3%. The supported Au [10] and Pd [11] monometallic catalysts and Au–Pd [12] bimetallic catalysts have also been used in benzyl alcohol oxidation exhibiting excellent catalytic activity. The use of inexpensive metals such as Cu, Mn and Ni-containing catalysts can offer a good alternative in comparison with the precious metals.

The use of MCM-41 as a catalyst support to immobilize metal complexes offers advantages as regular pore system which

\* Corresponding author. Tel.: +34 914887022; fax: +34 914888143.

E-mail address: [isabel.hierro@urjc.es](mailto:isabel.hierro@urjc.es) (I. del Hierro).

consists of a hexagonal array of unidimensional, hexagonally shaped pores, whose diameter can be varied systematically between 2 and 10 nm, highly specific surface area (up to  $1500 \text{ m}^2 \text{ g}^{-1}$ ) and a specific pore volume of up to  $1.3 \text{ mL g}^{-1}$ . MCM-41 as a catalyst support has been hardly reported in benzyl alcohol oxidation [13,14]. However, MCM-41 have been used in order to immobilize Cu(II) complexes. These materials have been used as a heterogeneous catalyst in several catalytic reactions. Corma and co-workers [15] have reported the heterogenization of Cu(II)-complexes with multidentate  $C_2$ -symmetry ligands derived from L-proline by anchoring or encapsulation onto the MCM-41 surface and into the cavities of Y zeolite. It was demonstrated that catalyst synthesized via anchoring of the complex obtained better catalytic results than the corresponding encapsulated yielding sulfoxides and epoxyalcohols with excellent yields and selectivity. Karandikar et al. [16] have immobilized copper Salen complexes onto an aminosilylated MCM-41 via tethering of the complex. Different characterization techniques reveal that the complex is monomolecularly attached to the walls of MCM-41 and shows evidence for adduct formation of the amino group through the axial coordination with the metal centre which enhances the catalytic activity for the liquid phase oxidation of olefins. Similar Schiff base complexes of copper have been grafted on the iodosilane modified surfaces of MCM-41 and MCM-48 [17] and used as catalysts for cyclooctene epoxidation.

Copper (II) acetate complex have been also immobilized onto a previously organofunctionalized MCM-41 with 3-aminopropyltrimethoxysilane via tethering process [18]. Copper (II) nitrate and copper acetylacetonate have been grafted onto MCM-41 employing different preparation techniques where the solvent and the copper solution concentration were varied [19]. Recently, Koner and co-workers [20] have reported anchoring of  $[\text{Cu}(\text{diamine})_2(\text{NO}_3)_2]$  onto the organically modified MCM-41. The amine group containing organic moiety (3-aminopropyl)triethoxysilane has been first anchored on the surface of MCM-41 via silicon alkoxide route.

In this paper, the metal precursors copper (II) ethylacetoacetate and copper (II) nitrate have been immobilized onto two different organofunctionalized MCM-41 materials with  $N^4$ -(3-(triethoxysilyl)propyl)pyrimidine-2,4,6-triamine (DAPyPTS) ligand. These organofunctionalized MCM-41 materials have been synthesized by post-synthesis and co-condensation methods. For comparison, two different media, organic and aqueous media, have been tested for the immobilization experiments of copper. Inexpensive copper containing catalysts exhibits a good catalytic activity in the solvent-free oxidation of benzyl alcohol with TBHP and  $\text{H}_2\text{O}_2$  as oxidants. The possibility of use  $\text{H}_2\text{O}_2$  as oxidant and the absence of solvent provide a well designed opportunity of using these catalysts for green chemistry proposal.

## 2. Experimental procedure

### 2.1. General remarks

The reactions carried out in organic medium were performed using standard Schlenk tube techniques under an atmosphere of dry nitrogen. Sulphuric acid 98% ( $M = 98.08 \text{ g mol}^{-1}$ ,  $d = 1.840 \text{ g mL}^{-1}$ ) was purchased from Panreac. Sodium silicate  $\text{SiO}_2 \cdot \text{NaOH}$  ( $M = 242.23 \text{ g mol}^{-1}$ ,  $d = 1.390 \text{ g mL}^{-1}$ ), tetraethyl orthosilicate (TEOS) and cetyltrimethylammonium bromide (CTAB) ( $M = 364.46 \text{ g mol}^{-1}$ ), were purchased from Sigma-Aldrich and used as supplied. The organic ligand  $N^4$ -(3-(triethoxysilyl)propyl)pyrimidine-2,4,6-triamine (DAPyPTS) was synthesized according to the procedure previously described by our group [21].  $\text{Cu}(\text{NO}_3)_2 \cdot 3\text{H}_2\text{O}$  ( $M = 241.6 \text{ g mol}^{-1}$ ) was

purchased from Panreac and copper (II) ethylacetoacetate (99%,  $M = 321.82 \text{ g mol}^{-1}$ ) was purchased from Strem Chemicals and both of them used as supplied. Benzyl alcohol ( $M = 108.14 \text{ g mol}^{-1}$ ,  $d = 1.045 \text{ g mL}^{-1}$ ) and tertbutylhydroperoxide (TBHP) (5–6 M decane) were purchased from Sigma-Aldrich and stored in presence of molecular sieves. Hydrogen peroxide 30% ( $M = 34.01 \text{ g mol}^{-1}$ ,  $d = 1.11 \text{ g mL}^{-1}$ ) was purchased from Sigma-Aldrich and used as supplied. Organic solvents, DMF, THF, dodecane, and heptane were purchased from SDS and distilled and dried before use according to conventional literature methods. Water was obtained from a Millipore Milli-Q system (Waters, USA).

### 2.2. Functionalization of the MCM-41 with DAPyPTS ligand

#### 2.2.1. Synthesis of DAPyPTS–MCM-41 hybrid material through grafting method

Synthesis of the hybrid material DAPyPTS–MCM-41 was previously reported by our group [21]. In a typical functionalizing experiment, 1 g sample of activated MCM-41 was suspended in 30 mL of dry DMF and the above mentioned pyrimidine silane ligand (DAPyPTS) (1 mL, 4 mmol) was added. The mixture was stirred for 48 h at room temperature and the resulting solid DAPyPTS–MCM-41 was obtained by filtration and washed with toluene (50 mL) and diethylether (50 mL). The solid material was dried under vacuum and stored under inert atmosphere.

#### 2.2.2. Synthesis of CoDAPyPTS–MCM-41 hybrid material through co-condensation method

In a typical synthesis, 1.1 g (3 mmol) of CTAB, 1.2 mL (62 mmol) of ammonium solution, 5.5 mL (0.024 mmol) of TEOS, 26 mL of distilled water and 0.24 g of DAPyPTS were added. The mixture was maintained under stirring for 24 h. The resulting gel was transferred to a Teflon-coated autoclave and heated at  $121^\circ\text{C}$  for 24 h. The solid produced was separated by suction filtration, washed several times with ethanol and dried at  $100^\circ\text{C}$  for 4 h. The surfactant was removed by extraction process with a reflux of ethanol for 24 h employing a soxhlet.

### 2.3. Synthesis of copper containing heterogenous catalysts

#### 2.3.1. Immobilization of copper in organic medium

Copper containing mesoporous materials were prepared by reaction of copper (II) nitrate or copper (II) ethylacetoacetate with the functionalized materials DAPyPTS–MCM-41 and CoDAPyPTS–MCM-41. In a typical experiment, copper (II) nitrate (0.48 g, 2 mmol) or copper (II) ethylacetoacetate (0.64 g, 2 mmol) was added to 2 g of DAPyPTS–MCM-41 or CoDAPyPTS–MCM-41 suspended in dry THF. The mixtures were stirred for 24 h at room temperature. The catalysts synthesized were obtained by filtering, washed several times with THF and dried under vacuum. The resulting materials were named as CuAc–DAPyPTS–MCM-41 and Cu–DAPyPTS–MCM-41 in case of using the functionalized material DAPyPTS–MCM-41 and copper (II) ethylacetoacetate or copper (II) nitrate, respectively. CuAc–CoDAPyPTS–MCM-41 and Cu–CoDAPyPTS–MCM-41 were labelled for the materials prepared by co-condensation CoDAPyPTS–MCM-41 with copper (II) ethylacetoacetate or copper (II) nitrate, respectively.

#### 2.3.2. Immobilization of copper in aqueous medium

Copper containing mesoporous materials were also prepared by reaction of an aqueous solution of copper (II) nitrate with the functionalized materials DAPyPTS–MCM-41 and CoDAPyPTS–MCM-41. In a typical experiment, copper (II) nitrate (0.48 g, 2 mmol) dissolved in distilled water was added to 2 g of DAPyPTS–MCM-41 or Co-DAPyPTS–MCM-41. The mixtures were stirred for 24 h at

room temperature. The materials synthesized were obtained by filtering, washed several times with water and dried at 130 °C. The resulting materials were named as Cu–DAPyPTS–MCM-41-W and Cu–CoDAPyPTS–MCM-41-W in case of using the functionalized materials DAPyPTS–MCM-41 or CoDAPyPTS–MCM-41, respectively.

#### 2.4. Catalytic benzyl alcohol oxidation

The synthesized hybrid materials were tested as catalyst for benzyl alcohol oxidation in order to determine their catalytic activity and selectivity. In a typical experiment, 2.6 mL (25 mmol) of benzyl alcohol, 3.27 mL or 6.67 mL (32 mmol) of H<sub>2</sub>O<sub>2</sub> or TBHP, respectively, 1 mL of heptane as standard internal and 0.25 g of catalyst are incorporated under nitrogen atmosphere to a reactor of a completely automated and monitored MultiMax™ parallel reactors system from Mettler Toledo. The reaction was monitored at 500 rpm stirring speed and maintained at 367 K for 4 h. In case of using H<sub>2</sub>O<sub>2</sub> as oxidant, the reaction time is reduced to 30 min due to its higher oxidant property. A Varian Chrompack CP-3380 gas chromatograph with a CP-SIL 8CB capillary column (25 m × 0.35 mm i.d., film thickness 1 μm) and a flame ionization detector (FID) was applied in the analysis of the samples of the catalytic test reaction. Heptane was used as internal standard to quantify the components in the samples.

#### 2.5. Techniques used in characterization

X-ray diffraction (XRD) patterns of the silicas were obtained on a Phillips Diffractometer model PW3040/00 X'Pert MPD/MRD at 45 kV and 40 mA, using Cu–Kα radiation ( $\lambda = 1.5418 \text{ \AA}$ ). N<sub>2</sub> gas adsorption–desorption isotherms were obtained using a Micromeritics TriStar 3000 analyzer, and pore size distributions were calculated using the Barret–Joyner–Halenda (BJH) model on the adsorption branch. Infrared spectra were recorded on a Nicolet-550 FT-IR spectrophotometer (in the region 4000–400 cm<sup>-1</sup>) as nujol mulls between polyethylene pellets and KBr disks. The DRUV–vis spectroscopic measurements were carried out on a Varian Cary-500 spectrophotometer equipped with an integrating sphere and polytetrafluoroethylene (PTFE) as reference, with  $d = 1 \text{ g cm}^{-3}$  and thickness of 6 mm. Proton-decoupled <sup>29</sup>Si MAS NMR spectra were recorded on a Varian-Infinity Plus 400 MHz Spectrometer operating at 79.44 MHz proton frequency (4 μs 90° pulse, 1024 transients, spinning speed of 5 MHz). Cross Polarization <sup>13</sup>C CP/MAS NMR spectra were recorded on a Varian-Infinity Plus 400 MHz Spectrometer operating at 100.52 MHz proton frequency (4 μs 90° pulse, 4000 transients, spinning speed of 6 MHz, contact time 3 ms, pulse delay 1.5 s). Elemental analysis (% C and % N) was performed by the Investigation Service of Universidad de Alcalá (Spain) using a CHNS analyser LECO-932 model. The copper content was determined by ICP-atomic emission spectroscopy (ICP-AES) using a Varian Vista AX model. Scanning electron micrographs and morphological analysis were carried out on a XL30 ESEM Philips.

### 3. Results and discussion

#### 3.1. Preparation and characterization of the DAPyPTS–MCM-41 and Co-DAPyPTS–MCM-41 hybrid materials

The preparation and characterization of the hybrid material DAPyPTS–MCM-41 have been previously reported by our group [21]. The organic compound was grafted on the MCM-41 surface by post-synthesis procedure. The ethoxy groups of the DAPyPTS compound were reacted with the hydroxyl groups to the

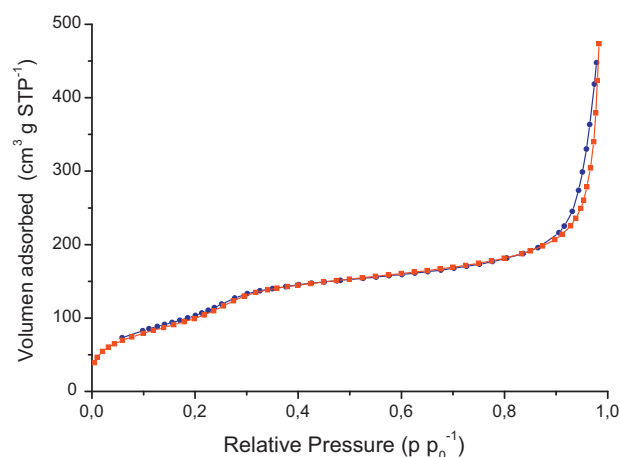


Fig. 1. Nitrogen adsorption–desorption isotherms of CoDAPyPTS–MCM-41.

MCM-41 surface liberating the corresponding alcohol. The material DAPyPTS–MCM-41 was obtained as a pale yellow solid.

As alternative route, the organic functional groups were incorporated into the MCM-41 framework by one-step “in situ” synthesis procedure, following the procedure reported by Li and co-workers [22], in the presence of DAPyPTS compound and using cetyltrimethylammonium bromide (CTAB) as surfactant template. The molar composition was used 0.12 CTAB, 0.5 NH<sub>3</sub>/H<sub>2</sub>O, 0.96 TEOS, 0.04 DAPyPTS, 58.24 H<sub>2</sub>O. Finally, the surfactant was removed by ethanol extraction to obtain the hybrid material termed as Co-DAPyPTS–MCM-41.

The nitrogen and carbon contents obtained from elemental analysis were 1.30% and 17.02%, respectively. The quantity of molecules attached to the mesoporous silica ( $L_0$ , mmol g<sup>-1</sup>) was calculated from the percentage of nitrogen in the CoDAPyPTS–MCM-41 material, using the following expression:

$$L_0 \left( \frac{\text{mmol}}{\text{g}} \right) = \frac{\%N \cdot 2}{\text{nitrogen atomic weight}}$$

The pyrimidine based ligand loading was found to be 0.2 mmol g<sup>-1</sup> for CoDAPyPTS–MCM-41 on the basis of nitrogen content measurements. Taking into account  $L_0$  and  $S_{\text{BET}}$  of the mesoporous silica, the average surface density ( $d$ , molecules nm<sup>-2</sup>) of the attached molecules and the average intermolecular distance ( $l$ , nm) were calculated [23]. The obtained values were  $d = 0.7$  molecules nm<sup>-2</sup> and  $l = 1.2$  nm.

The mesostructure of the hybrid material was confirmed by nitrogen adsorption–desorption technique and X-ray diffraction. The BET specific area of the material CoDAPyPTS–MCM-41 was determined by N<sub>2</sub> adsorption–desorption isotherm. Mesoporous characteristic type IV isotherm according to the IUPAC classification was obtained and it has an H1 hysteresis loop that is representative of mesoporous cylindrical or rod-like pores (Fig. 1). The hybrid material displayed a well-resolved pattern at low  $2\theta$  values with a very sharp (100) diffraction peak characteristic of a mesoporous structure.

Combining N<sub>2</sub> adsorption–desorption and X-ray results, different parameters can be calculated (Table 1). Comparing the materials synthesized by post-synthesis and co-condensation method, the latter presents higher pore diameter (from 12 to 71 Å) and specific surface area,  $S_{\text{BET}}$  (from 246 to 598 m<sup>2</sup> g<sup>-1</sup>) values. This is consistent with the behaviour previously describe in literature. For instance, Jaroniec and co-worker [24] obtained a difference of 33–76 Å pore diameter and 112–728 m<sup>2</sup> g<sup>-1</sup>  $S_{\text{BET}}$ , in the post-synthesis and co-condensation preparation of MCM-41 functionalized with 2,5-dimercapto-1,2,3-thiazole ligand, respectively.

**Table 1**  
Results of the structural characterization obtained for CoDAPyPTS–MCM-41 and DAPyPTS–MCM-41 materials and copper-containing materials.

Material	$S_{\text{BET}}$ ( $\text{m}^2 \text{g}^{-1}$ )	Pore volume ( $\text{cm}^3 \text{g}^{-1}$ )	Pore diameter ( $\text{Å}$ )	$d_{100}$ ( $\text{Å}$ )
DAPyPTS–MCM-41 <sup>a</sup>	246	0.26	12	34
CoDAPyPTS–MCM-41	597	0.74	71	65
CuAc–DAPyPTS–MCM-41	182	0.22	10	41
Cu–DAPyPTS–MCM-41	196	0.23	11	32
Cu–CoDAPyPTS–MCM-41	332	0.35	42	58
CuAc–CoDAPyPTS–MCM-41	245	0.30	41	69
Cu–DAPyPTS–MCM-41-W	205	0.25	11	–
Cu–CoDAPyPTS–MCM-41-W	297	0.35	44	–

<sup>a</sup> Ref. [21].

Post synthesis modification process after forming the mesoporous structure introduces an inherent disorder and decreases the size of mesopores, but not results in the collapse of the pore structure of mesoporous materials. In fact, the pore is reduced when the organic molecules are immobilized into the MCM-41 channels during the modification process. On the other hand, in the co-condensation method, when the silica–surfactant composites are formed in the micellar solution, hydrophobic interactions between the terminal organic moiety of the organoalkoxysilane and the long alkyl chain of the surfactant would be interrupted by the presence of hydrophilic amino groups resulting in a large  $d_{100}$  spacing [25]. Udayakumar et al. [26] suggested an interesting conclusion; as the concentration of organic ligand in the co-condensation method increases, the  $S_{\text{BET}}$  and the pore diameter present higher values. This behaviour shows the importance of the organic ligand incorporation method in the final structural parameters of the hybrid material.

The hybrid material was also characterized by <sup>29</sup>Si and <sup>13</sup>C MAS NMR. <sup>29</sup>Si MAS NMR spectrum of CoDAPyPTS–MCM-41 is shown in Fig. 2. The peaks at –110 and –101 ppm assigned to Q<sup>4</sup> siloxane ((SiO)<sub>4</sub>Si) and Q<sup>3</sup> silanol sites ((SiO)<sub>3</sub>SiOH), respectively from TEOS. T<sup>2</sup> [SiR(OSi)<sub>2</sub>(OR')] and T<sup>3</sup> [(OSi)<sub>3</sub>SiR] sites appear at –65 and –69 ppm, respectively, confirming that pyrimidine based silane groups are well preserved after organofunctionalization and extraction of template.

In Fig. 3a it is shown the <sup>13</sup>C MAS NMR spectrum of CoDAPyPTS–MCM-41. The three signals from the three carbon atoms present in the alkyl chain appears at 11, 24 and 39 ppm for ≡Si–CH<sub>2</sub>–, CH<sub>2</sub>–CH<sub>2</sub>–CH<sub>2</sub>– and –CH<sub>2</sub>–O, respectively. The signal attributed to aromatic carbons C<sub>4</sub>N<sub>2</sub> of pyrimidine ligand appears at 165 ppm.

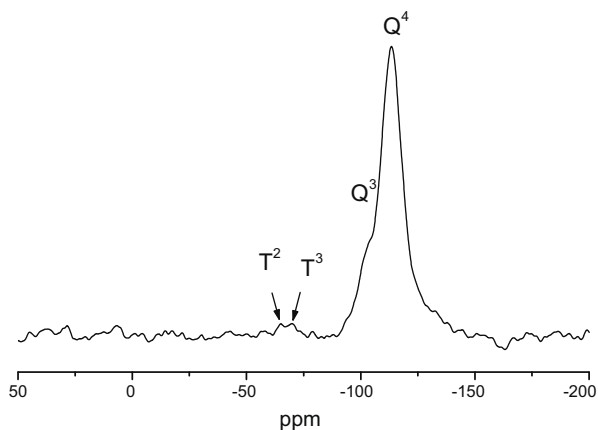


**Fig. 2.** <sup>29</sup>Si MAS NMR spectrum of CoDAPyPTS–MCM-41.

### 3.2. Preparation and characterization of the copper-containing catalysts

#### 3.2.1. Immobilization of copper on modified MCM-41 materials in organic medium

Copper precursors react with the amino-pyrimidine functionalized materials DAPyPTS–MCM-41 and CoDAPyPTS–MCM-41 following Scheme 1. To prepare the copper functionalized materials, copper nitrate or copper (II) ethylacetoacetate, was dissolved in THF and added to the functionalized mesoporous silicas. The suspension was maintained 24 h at room temperature under stirring. The blue and green solids obtained, respectively, were recovered by filtration and washed several times with THF. In this way four different materials were obtained and labelled as Cu–DAPyPTS–MCM-41, CuAc–DAPyPTS–MCM-41, Cu–CoDAPyPTS–MCM-41 and CuAc–CoDAPyPTS–MCM-41 where “CuAc” represents materials prepared using copper ethylacetoacetate and “Cu” symbolizes materials synthesized from copper nitrate as metallic precursors.

The mesostructures of copper MCM-41 materials were confirmed by powder X-ray diffraction. As can be seen in Fig. 4 the mesoporous structure of parent MCM-41 is preserved after immobilization. A well resolved pattern with a very sharp (100)

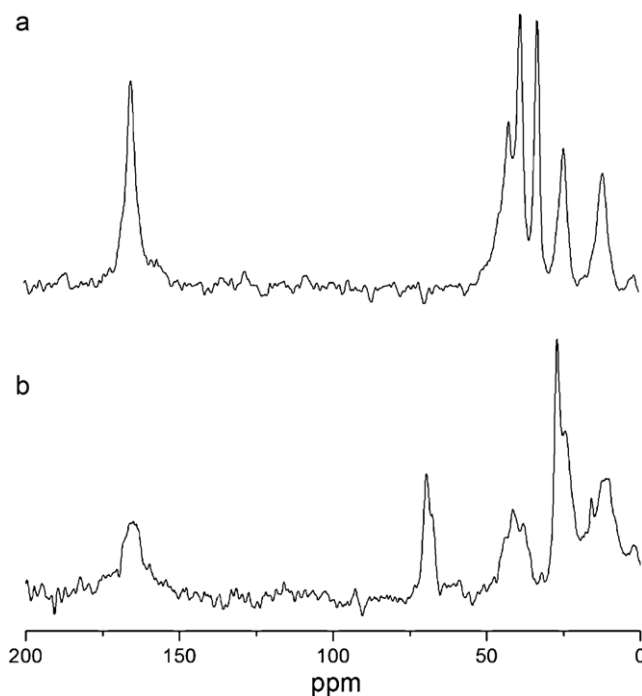
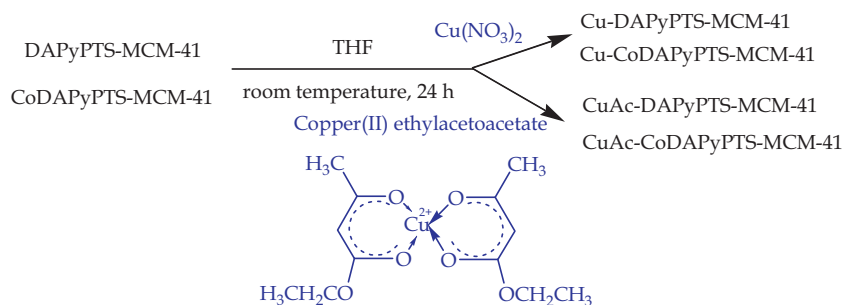


**Fig. 3.** <sup>13</sup>C MAS NMR spectra of (a) CoDAPyPTS–MCM-41 and (b) CuAc–CoDAPyPTS–MCM-41.





**Scheme 1.** Synthesis of copper-containing materials in organic medium.

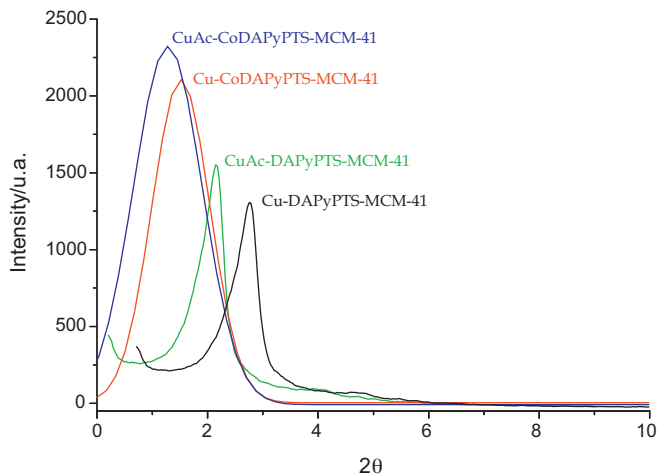


**Fig. 4.** Powder X-ray diffraction patterns of copper-containing materials.

diffraction peak is obtained for the four materials indicating a good mesoscopic order. The physical parameters of the nitrogen isotherms, such the surface area ( $S_{\text{BET}}$ ), total pore volume and average pore diameter for copper-containing materials are shown in Table 1.

Figs. 5 and 6 show FT-IR spectra of copper heterogenized samples, following the immobilization of copper (II) nitrate or copper (II) ethylacetoacetate onto DAPyPTS-MCM-41 and CoDAPy-MCM-41 materials. All the graphs show typical adsorption bands of the amino pyrimidine silane ligand at ca.  $2970\text{--}2850\text{ cm}^{-1}$ , associated with the  $\nu(\text{CH}_2)$  stretching and  $\nu(\text{CH}_2)$  bending vibrations from incorporated organic ligand, respectively. The spectra also present

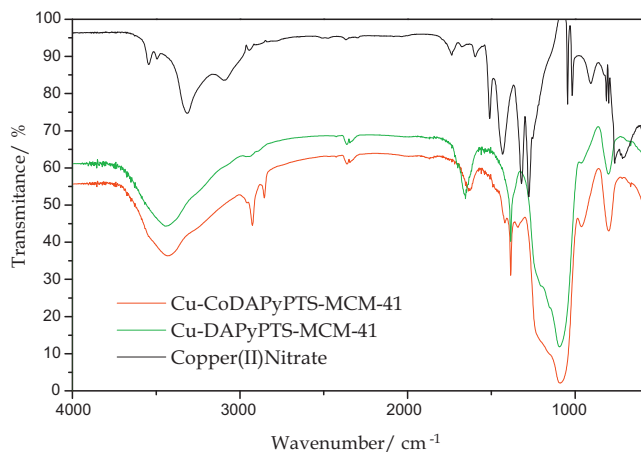


**Fig. 5.** FTIR spectra of copper (II) nitrate precursor and, Cu-CoDAPyPTS-MCM-41 and Cu-DAPyPTS-MCM-41 hybrid materials.

adsorption bands in the range  $1375\text{--}1575\text{ cm}^{-1}$  assigned to the the skeleton stretching vibration of  $\nu(\text{C-N})$  heterocyclic rings. FT-IR spectra of CuAc-DAPyPTS-MCM-41 and CuAc-CoDAPyPTS-MCM-41 materials (Fig. 5) show a strong absorption band at  $1383\text{ cm}^{-1}$  which corresponds to the stretching vibrations associated with the  $\text{N=O}$  bond of the  $\text{NO}_3$  group [27].

FT-IR spectrum of copper (II) ethylacetoacetate (Fig. 6) shows strong bands at  $1590$  and  $1529\text{ cm}^{-1}$  assigned to  $\nu(\text{C-C})$  coupled with  $\nu(\text{C-O})$  bond and  $\nu(\text{C-O})$  coupled with  $\nu(\text{C-C})$ , respectively. After immobilization, none of the bands due to the free copper precursor can be found in both materials CuAc-DAPyPTS-MCM-41 and CuAc-CoDAPyPTS-MCM-41, a direct indication that a change in the coordination sphere of the complex has taken place. In this context, the new bands/shoulders may be attributed to the anchored complex and assigned to stretching vibrations associated with the new  $\text{C=N}$  bond formed by Schiff condensation reaction between the amine groups of the incorporated silane ligand and the  $\text{C=O}$  group from the coordinated  $\beta$ -diketone ligand, as previously described by Silva et al. [28].

The diffusion reflectance ultraviolet visible absorption spectra of Cu(II) complexes grafted were scanned in the  $200\text{--}800\text{ nm}$  range (Fig. 7). DRUV-Vis spectra of copper nitrate and copper ethylacetoacetate show a broad band at  $600\text{--}800\text{ nm}$  assigned to d-d transition of  $\text{Cu}^{2+}$ . Upon heterogenization onto amino functionalized MCM-41 new bands associated to ligand and/or from metal to ligand charge transfer transition observed at lower wavelength tend to obscure the very weak d-d transitions, as clearly evidence the DRUV-vis spectra for Cu-DAPy-MCM-41 and Cu-CoDAPyMCM-41 materials. The energies and the very low intensities of these d-d transitions compared favourably

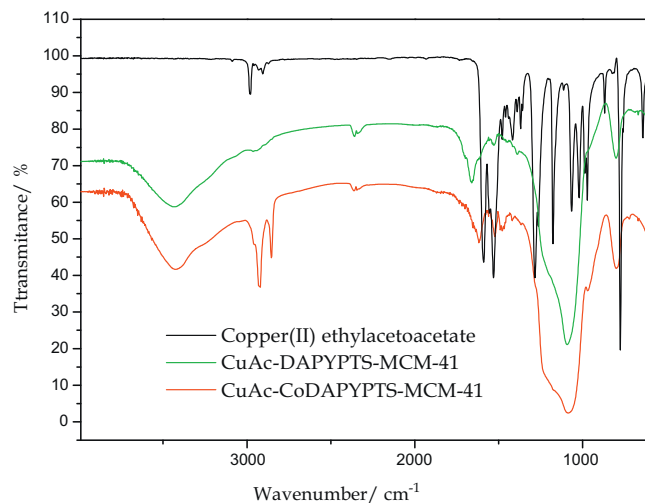


**Fig. 6.** FTIR spectra of copper (II) ethylacetoacetate precursor and, CuAc-DAPyPTS-MCM-41 and CuAc-CoDAPyPTS-MCM-41 hybrid materials.

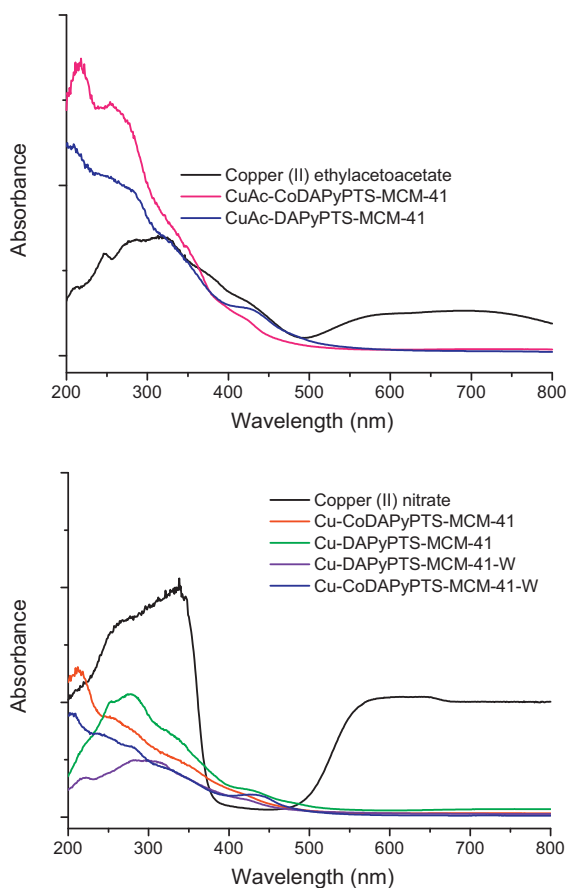


Fig. 7. DRUV-vis spectra of copper-containing materials.

with similar distorted octahedral systems [29]. In addition, the copper materials obtained by reaction of the ligand amine groups and ethylacetoacetate precursor show bands at 218 and 240 nm characteristics of the  $\beta$ -diketone ligand and at 320 and 426 nm due to charge transfer bands, in accordance with similar square planar complexes found in bibliography [30,31].

The  $^{13}\text{C}$  MAS NMR spectrum of CuAc-CoDAPyPTS-MCM-41 is shown in Fig. 3b. In the spectrum appear new peaks at 16, 24, 59 and 69 ppm which are attributed to the immobilization of copper (II) ethylacetoacetate onto CoDAPy-MCM-41 material.

Inductively coupled plasma-atomic emission spectroscopy (ICP-AES) and scanning electron microscope (SEM) with energy-dispersive X-ray (EDX) analysis are used in the quantification of the amount of copper presented in each synthesized catalyst. As can be seen in Table 2, the amount of copper analysed by ICP-AES concurs with SEM-EDX the results obtaining relatively similar values. Considering that copper (II) salts are anchored via the incorporated ligand DAPyPTS into de mesoporous silica, the anchoring efficiency of copper towards the linker can be estimated taking into account the amount of incorporated ligand and copper loading. The amount of incorporated ligand is 0.3 and 0.2  $\text{mmol g}^{-1}$  for DAPyPTS-MCM-41 and CoDAPyPTS-MCM-41 materials, respectively. So as can be observed in Table 2, the materials synthesized by immobilization of copper (II) ethylacetoacetate present high anchored efficiency, providing complexes with nearly 1:2 stoichiometry. The sterical requirements imposed by the copper precursor can control the complexes formation with the amine pyrimidine ligand.

On the contrary, when copper (II) nitrate is employed as copper precursor, significant differences are found. The material Cu-CoDAPyPTS-MCM-41 synthesized from CoDAPyPTS

-MCM-41 obtained by co-condensation method loads remarkably higher amount of copper,  $0.9 \text{ mmol g}^{-1}$ , in comparison to the amount of copper loading of  $0.4 \text{ mmol g}^{-1}$  obtained with the material Cu-DAPyPTS-MCM-41, synthesized from material DAPyPTS-MCM-41 prepared by post-synthesis procedure. Comparison between the Cu anchoring efficiency of both materials shows that CoDAPyPTS-MCM-41 enhanced the copper immobilization. Nevertheless, the higher values obtained for the anchoring of copper nitrate onto CoDAPyPTS-MCM-41 compared to that of DAPyPTS-MCM-41 cannot be attributed solely to the amount of grafted ligand onto CoDAPyPTS-MCM-41. These results suggest at the first sight, that some direct anchoring cannot be excluded in Cu-CoDAPyPTS-MCM-41 functionalized material. Many authors have previously observed [32,33] and Shanks and co-workers [34] demonstrated that, in case of post-synthesis procedure, the organic compounds are located, preferentially, outside of the mesoporous particle and at the pore mouth of the materials, while co-condensation methods promote well-dispersed organic compounds within the pores, increasing availability of the corresponding amino pyrimidine ligands.

Scanning electron microscopy with energy dispersive X-ray microanalysis (SEM/EDX) mapping technique is employed to investigate the copper distribution. Scanning electron microscope (SEM) of the samples is carried out in order to observe different superficial morphologies of the material depending of the synthetic process used. As can be seen in Fig. 8a and b, lower particle size is obtained when grafting process is employed instead of co-condensation. This means that the incorporation of the organic ligand during the synthetic process of the MCM-41 interrupts the formation of small particles of the materials. Furthermore, EDX analysis (Fig. 8c) Cu K and L lines' presence indicates the evidence of incorporation of copper on the hybrid materials.

EDX maps show the copper distribution along the hybrid materials surface (see Fig. 9). The bright points represented the signal of copper element from the solid sample, copper are spread over the surfaces of hybrid materials. As can be seen, with different copper precursors and different techniques employed in the hybrid materials synthesis, grafting or co-condensation, copper is distributed uniformly on the surface of all materials. This observation supports the idea that the incorporation of copper onto the silica framework, at the concentrations used here, does not produce large particles of copper oxide species.

Taking into account the experimental and bibliographic [35] evidences, the proposed structures for the catalyst synthesized using different copper precursors are shown in Fig. 10a and b. Ethylacetoacetate could be irreversibly immobilized onto the amine-pyrimidine functionalized MCM-41 through Schiff condensation between the surface amine groups and the oxygen atoms of the copper  $\beta$ -diketonate ligand, leading to a tetracoordinated copper with an equatorial  $\text{O}_3\text{N}$  coordination sphere. Herein, when copper nitrate is used, the formation of dative bonds with the donor nitrogen atoms of the ligands is proposed. The coordination sphere is saturated with the nitrate anions with bidentate coordination [36,37] and presumably by some solvent or water molecules present in the medium.

### 3.2.2. Immobilization of Copper on modified MCM-41 materials in aqueous medium

The DAPyPTS-MCM-41 hybrid material has previously been explored by our group in adsorption capacity to remove heavy metals such nickel, copper and cobalt [21]. The results indicated that this material has successfully selectivity in the removal and preconcentration of copper from water. Following this, immobilization of copper (II) nitrate was also carried out in aqueous medium. Copper (II) nitrate was dissolved in water and added to the amino-functionalized materials DAPyPTS-MCM-41

**Table 2**

Copper determination by ICP-AES and by SEM-EDX and molar ratio Cu/DAPyPTS of the copper-containing materials.

Catalyst	Cu (%)	Cu (mmol g <sup>-1</sup> )ICP-AES	Cu (mmol g <sup>-1</sup> )SEM-EDX	Molar ratioCu/DAPyPTS
CuAc-DAPyPTS-MCM-41	3.0	0.5	0.2	1.7:1
Cu-DAPyPTS-MCM-41	2.8	0.4	0.3	1.3:1
Cu-CoDAPyPTS-MCM-41	5.9	0.9	0.8	4.5:1
CuAc-CoDAPyPTS-MCM-41	3.1	0.5	0.3	2.5:1

or CoDAPyPTS-MCM-41 in order to synthesize novel copper-containing catalysts. The green solids were recovered by filtration, washed several times with water and dried at 130 °C. In this way the materials were labelled as Cu-DAPyPTS-MCM-41-W and Cu-CoDAPyPTS-MCM-41-W where "W" indicates that the material was synthesized in aqueous medium.

The <sup>1</sup>H NMR spectrum of Cu-CoDAPyPTS-MCM-41-W is shown in Fig. 11. The signals corresponding to the alkyl carbon chain, methylene groups appear at 0.37, 1.60 and 3.19 ppm, respectively. The amino groups exhibit a broad signal in the range 8.0–9.0 ppm.

Inductively coupled plasma-atomic emission spectroscopy (ICP-AES) and scanning electron microscope (SEM) with energy-dispersive X-ray (EDX) analysis are used in the quantification of the amount of copper presented in both materials. Again, both techniques show similar values. As can be seen in Table 2 the material synthesized by immobilization of copper (II) nitrate onto CoDAPyPTS-MCM-41 achieves remarkably higher amount of copper loadings 0.5 mmol g<sup>-1</sup> in comparison to 0.1 mmol g<sup>-1</sup> obtained with the material DAPyPTS-MCM-41. This tendency is also observed when using organic medium. Other factor that must

be considered in order to explain this behaviour is the hydrophobicity provided by the organic ligand and the lower surface area and pore volume of DAPyPTS-MCM-41 when compared it to CoDAPyPTS-MCM-41. A representation of the proposed structure of the Cu-CoDAPyPTS-MCM-41-W material can be observed in Fig. 9c.

In order to determine the dispersion of the copper immobilized onto the hybrid material scanning electron microscopy with energy dispersive X-ray microanalysis (SEM/EDX) mapping technique is used. Fig. 12 shows SEM/EDX maps of Cu-DAPyPTS-MCM-41-W and Cu-CoDAPyPTS-MCM-41-W. The bright spots in the EDX mapping indicate that both materials present similar pattern of copper distribution independently on parent material synthesis procedure.

### 3.3. Benzyl alcohol oxidation with catalysts synthesized in organic media

The catalytic oxidation of benzyl alcohol is shown in Scheme 2. As can be seen, different products can be obtained such as benzaldehyde, benzoic acid and benzyl benzoate. In our experiments

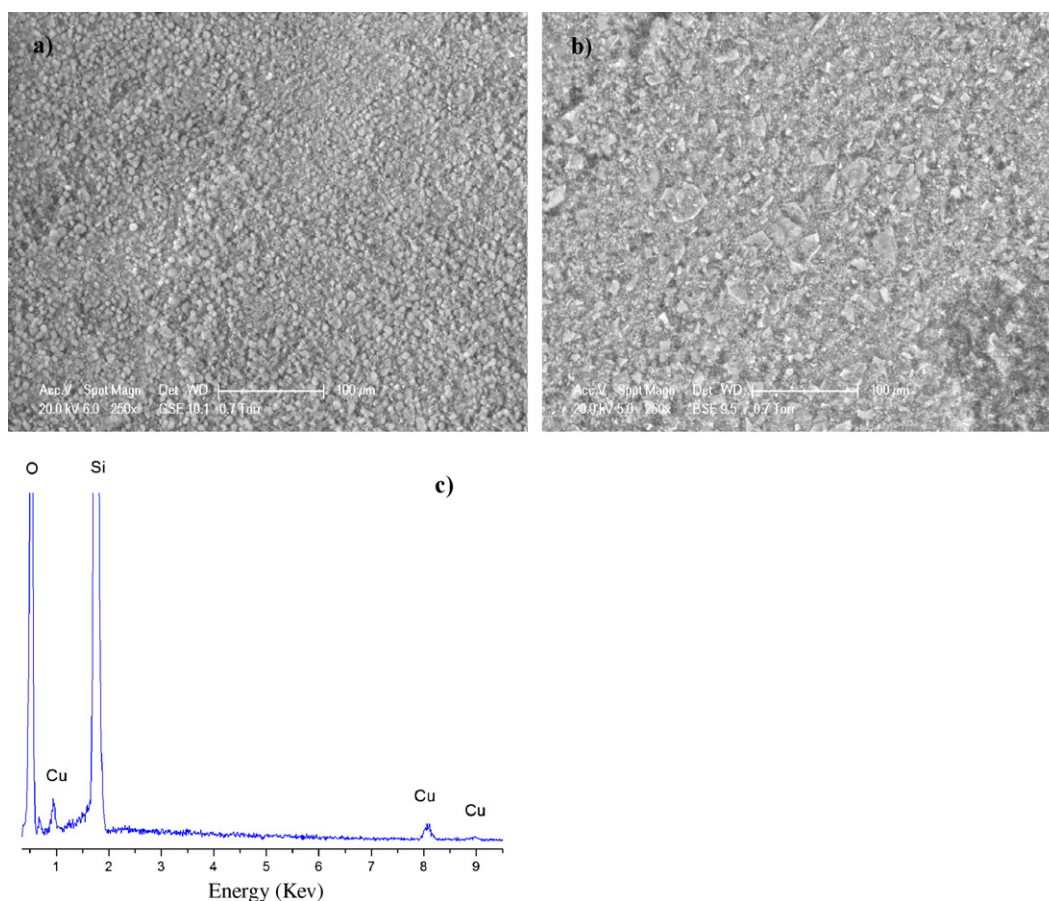


**Fig. 8.** SEM analysis (a) SEM image of Cu-DAPyPTS-MCM-41, (b) SEM image of Cu-CoDAPyPTS-MCM-41 and (c) EDX spectrum of Cu-CoDAPyPTS-MCM-41.



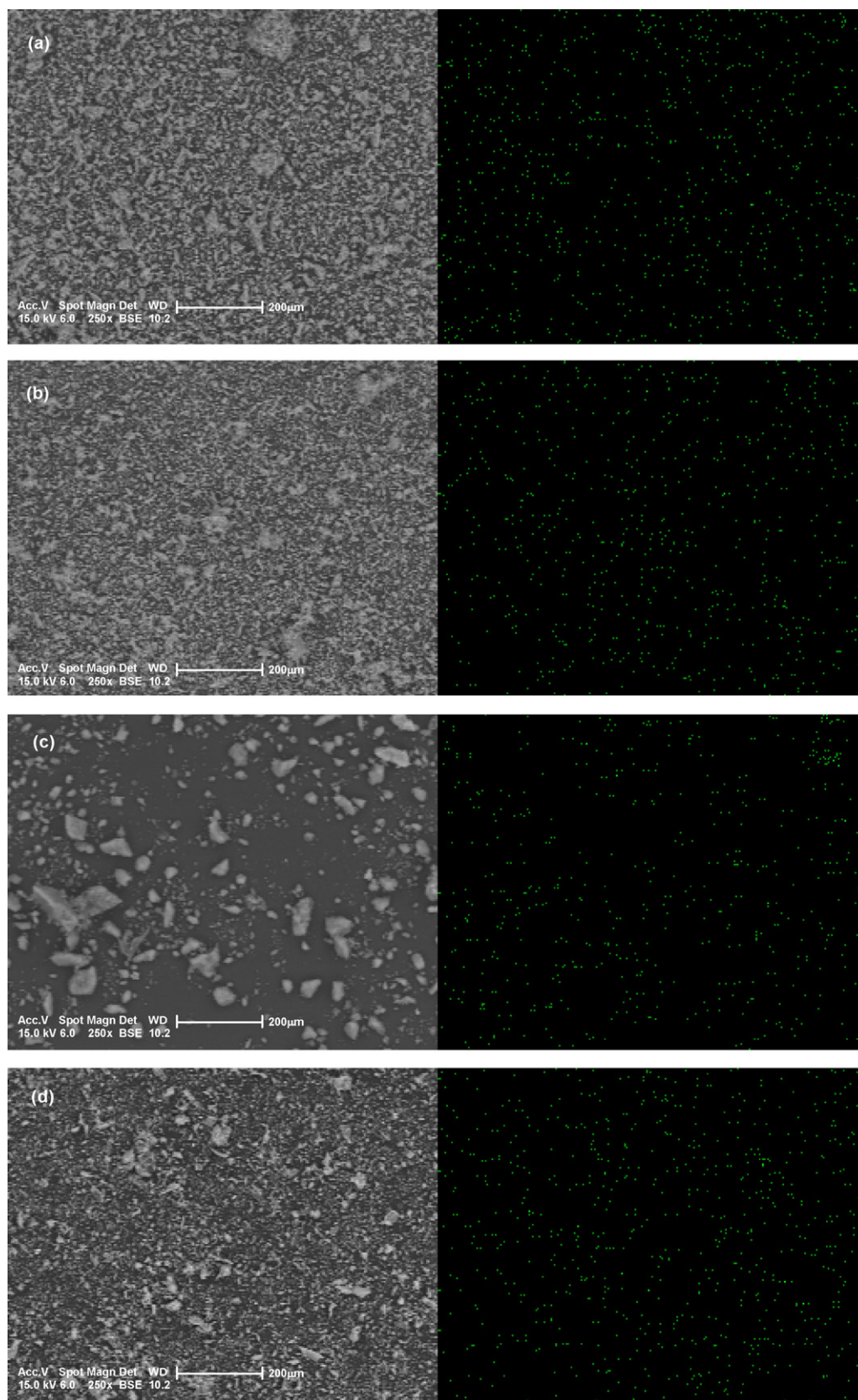


**Fig. 9.** Mapping of the copper containing of the (a) Cu-DAPyPTS-MCM-41, (b) CuAc-DAPyPTS-MCM-41, (c) Cu-CoDAPyPTS-MCM-41 and (d) CuAc-CoDAPyPTS-MCM-41 materials.



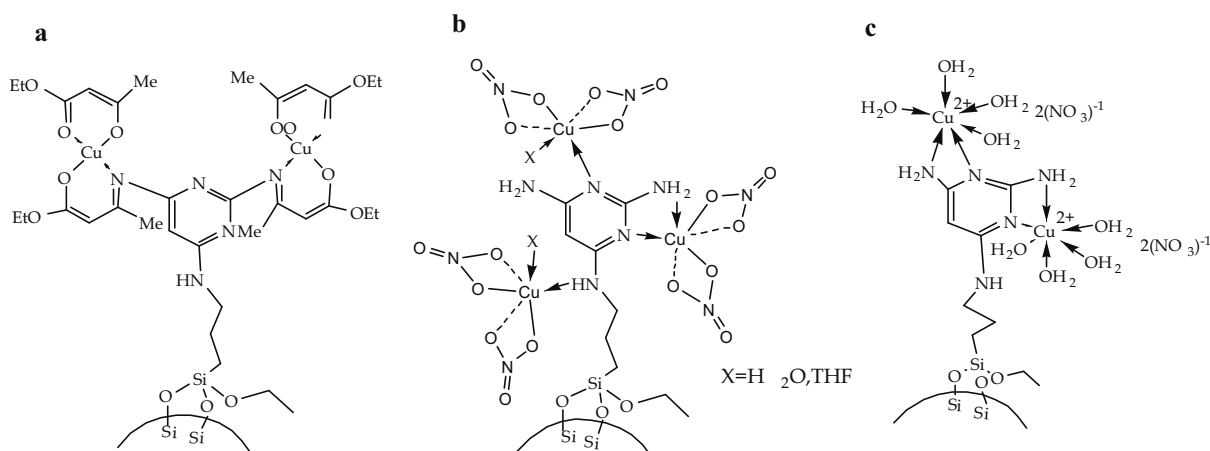
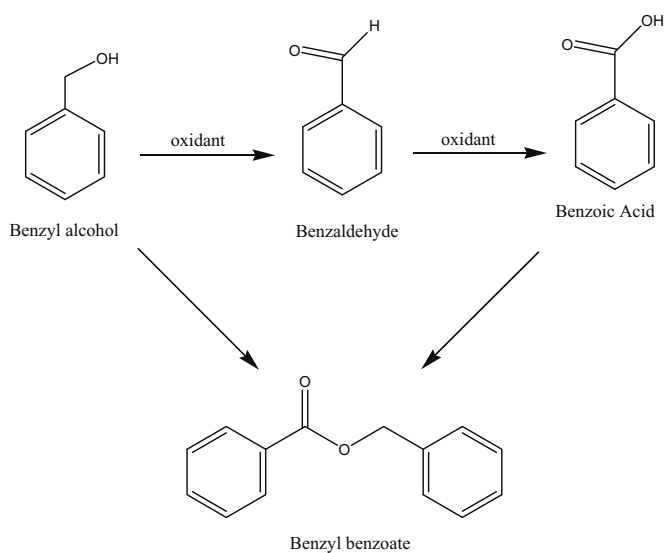


**Fig. 10.** Schematic representations of the different copper-containing materials prepared by immobilization of (a) copper (II) ethylacetoacetate in organic medium, (b) copper (II) nitrate in organic medium and (c) copper (II) nitrate in aqueous medium.



**Scheme 2.** Representation of the benzyl alcohol oxidation reaction and its products.

benzyl benzoate is not formed during the catalytic reactions and benzoic acid is obtained as secondary product. In addition, it has been observed in control experiments that the reaction does not proceed in the absence of catalyst and the conversion of benzyl alcohol on pure DAPyPTS–MCM-41, CoDAPyPTS–MCM-41 is very low, what demonstrate that the copper species are the effective

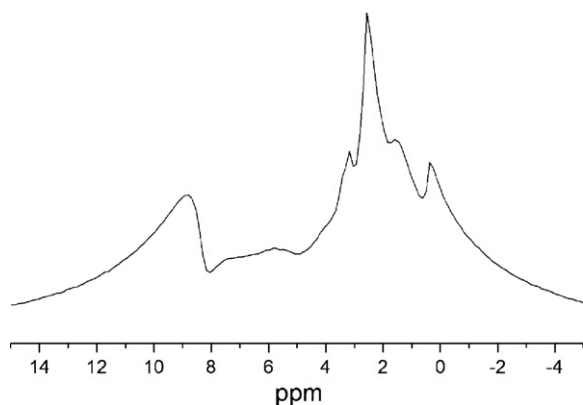


**Fig. 11.**  $^1\text{H}$  MAS NMR spectrum of Cu–CoDAPyPTS–MCM-41–W.

active sites for the oxidation of benzyl alcohol. All the reactions are carried out under inert atmosphere solvent-free providing an advantage front the others that employ organic solvents such as benzene or acetonitrile in the reaction medium (see Section 1).

### 3.3.1. Benzyl alcohol oxidation with TBHP

The catalytic activity of the immobilized copper catalysts for the oxidation of benzyl alcohol is studied with tertbutylhydroperoxide, TBHP, as oxidant. As a typical reaction procedure, oxidation experiments are performed as follows: 25 mmol of benzyl alcohol, 32 mmol of TBHP and 0.25 g of copper catalyst, are stirred and heated at 367 K for 4 h.

Oxidation of benzyl alcohol with TBHP mainly produces benzaldehyde with different conversions (35–54%) and selectivities (46–97%). CuAc–DAPy–MCM-41 catalyst exhibits high selectivity to benzaldehyde (97%) and moderate conversion (35%) (Table 3). Recently, Hamza et al. [10] have reported copper phthalocyanine immobilized on MCM-41 material in the oxidation of benzyl alcohol at 373 K for 4 h obtaining 30% of conversion and using dioxane as solvent. The tendency followed by the catalytic activity can be directly related to the amount of copper loading of the materials prepared in organic media, as can be seen in Table 3. Cu–CoDAPyPTS–MCM-41 with the highest amount of copper immobilized ( $0.9 \text{ mmol g}^{-1}$ ) led to the highest conversion value (54%).

If turn-over frequency values [TOF = moles of benzyl alcohol converted per mole of copper per hour] are compared (Table 3) Cu–DAPyPTS–MCM-41 is that which present the better activity results with 23 TOF value. Valodkar et al. [7] carried out the oxidation with TBHP and using copper (II)–L-valine complexes anchored on cross-linked styrene–divinyl benzene polymer achieving the highest activity catalytic with 22 TOF value.

### 3.3.2. Benzyl alcohol oxidation with $\text{H}_2\text{O}_2$

The catalytic activity of the immobilized copper catalysts, for the oxidation of benzyl alcohol was also studied with hydrogen peroxide as oxidant agent. Hydrogen peroxide is the preferred oxidant in zeolite systems, since it is highly mobile in the pores due to their smaller size. Furthermore, it is cheaper and sufficiently environment-friendly to be used on a commercial scale. As a typical reaction procedure, oxidation experiments are performed as follows: 25 mmol of benzyl alcohol, 32 mmol of  $\text{H}_2\text{O}_2$  and 0.25 g of copper catalyst, are stirred and heated at 367 K for just 30 min.  $\text{H}_2\text{O}_2$  is better oxidant than TBHP, and rapidly conversion 39% for Cu–DAPyPTS–MCM-41 is obtained in 30 min (Table 4). These results are in agreement with other copper catalyst previously

**Table 3**  
Catalytic results for benzyl alcohol oxidation employing THBP as oxidant.<sup>a</sup>

Catalyst	Conversion <sup>b</sup> (%)	Selectivity <sup>c</sup> (%)	TOF (h <sup>-1</sup> )	Cu (mmol g <sup>-1</sup> )
DAPyPTS–MCM-41	0.5	–	–	–
CoDAPyPTS–MCM-41	1.2	–	–	–
CuAc–DAPyPTS–MCM-41	35	97	18	0.5
Cu–DAPyPTS–MCM-41	36	86	23	0.4
Cu–CoDAPyPTS–MCM-41	54	46	15	0.9
CuAc–CoDAPyPTS–MCM-41	36	81	18	0.5
Cu–DAPyPTS–MCM-41-W	62	32	155	0.1
Cu–CoDAPyPTS–MCM-41-W	58	42	29	0.5

<sup>a</sup> Reaction conditions: catalyst: 0.25 g, benzyl alcohol: 25 mmol, TBHP: 32 mmol, solvent: solvent free system, internal standard: 1 mL heptane, temperature: 367 K, time: 4 h.

<sup>b</sup> Benzyl alcohol conversion.

<sup>c</sup> Selectivity towards benzaldehyde.

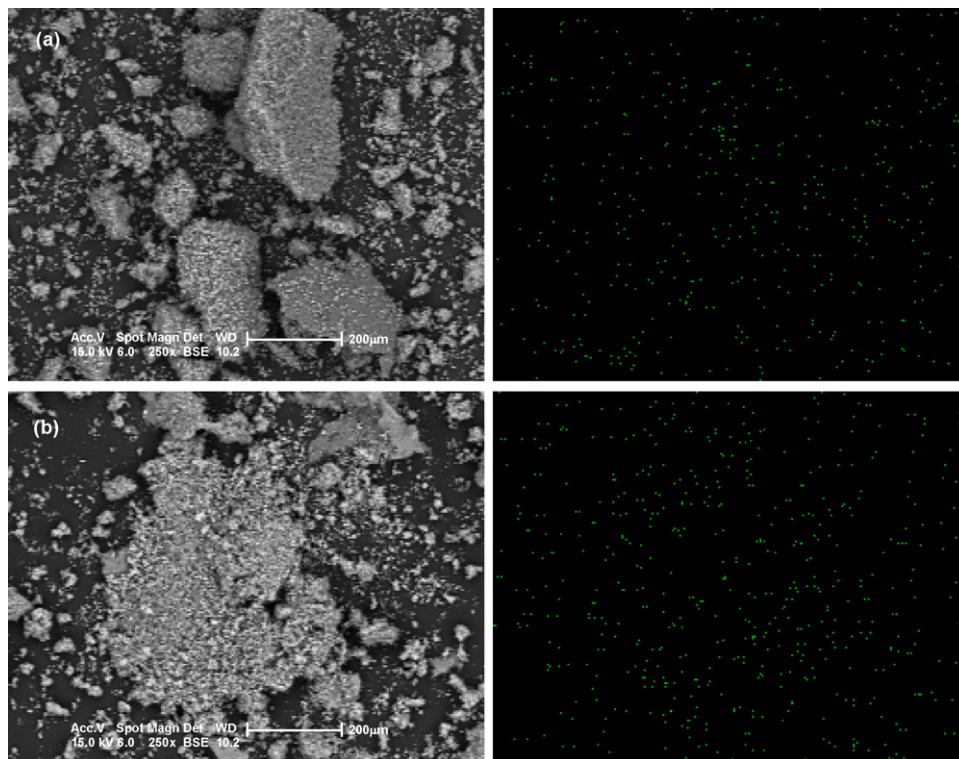


**Fig. 12.** Mapping of the copper containing of the (a) Cu–DAPyPTS–MCM-41-W and (b) Cu–CoDAPyPTS–MCM-41-W materials.

**Table 4**  
Catalytic results for benzyl alcohol oxidation employing H<sub>2</sub>O<sub>2</sub> as oxidant.<sup>a</sup>

Catalyst	Conversion <sup>b</sup> (%)	Selectivity <sup>c</sup> (%)	TOF (h <sup>-1</sup> )	Cu (mmol g <sup>-1</sup> )
DAPyPTS–MCM-41	0.8	–	–	–
CoDAPyPTS–MCM-41	1.5	–	–	–
CuAc–DAPyPTS–MCM-41	20	35	80	0.5
Cu–DAPyPTS–MCM-41	39	45	195	0.4
Cu–CoDAPyPTS–MCM-41	32	56	71	0.9
CuAc–CoDAPyPTS–MCM-41	24	75	96	0.5
Cu–DAPyPTS–MCM-41-W	21	45	420	0.1
Cu–CoDAPyPTS–MCM-41-W	23	27	92	0.5
Cu–DAPyPTS–MCM-41-W <sup>d</sup>	19	32	380	0.1
Cu–CoDAPyPTS–MCM-41-W <sup>d</sup>	19	21	76	0.5
Cu–DAPyPTS–MCM-41-W <sup>e</sup>	17	25	340	0.1
Cu–CoDAPyPTS–MCM-41-W <sup>e</sup>	15	17	60	0.5

<sup>a</sup> Reaction conditions: catalyst: 0.25 g, benzyl alcohol: 25 mmol, H<sub>2</sub>O<sub>2</sub>: 32 mmol, solvent: solvent free system, internal standard: 1 mL heptane, temperature: 367 K, time: 30 min.

<sup>b</sup> Benzyl alcohol conversion.

<sup>c</sup> Selectivity towards benzaldehyde.

<sup>d</sup> Reused material (first run).

<sup>e</sup> Reused material (second run).

reported, as example, Cu(II) complexes with dimethylglyoxime and Me<sub>2</sub>salen (*N,N'*-ethylenbis(7-methylsalicylideneamine)) ligands encapsulated in Y zeolite [4], which show conversion values in the range 30–52% but higher times (8 h). Copper containing hydrotalcite-like solid catalysts [8] show 41% of conversion in 5 h under solventless and using molecular oxygen as oxidant.

Cu–DAPyPTS–MCM-41 material synthesized by post-synthesis procedure provides highest benzyl alcohol conversion value and a moderate selectivity (45%) towards benzaldehyde when H<sub>2</sub>O<sub>2</sub> is used (Table 4). Some authors justified this behaviour because of the fact that post-synthesis procedure favours the encounter among substrate, catalytic active site and oxidant. In case of co-condensation, higher metal complexes incorporation results are usually obtaining, but at the same time, the availability of the active sites is lower. For instance, Yang et al. [38] prepared two different types of sulfonic acid functionalized mesoporous silicas first via co-condensation and second by grafting and tested them in the catalytic esterification of acetic acid with ethanol. The published results show that the catalytic activity of the co-condensation catalysts was one third of that of the grafting catalysts. The authors justified this result on basis on the easily accessible catalytic active species of the grafted materials, which are preferentially located on the external surface or near the pore mouth.

#### 3.4. Benzyl alcohol oxidation with catalysts synthesized in aqueous media

The catalysts Cu–DAPyPTS–MCM-41-W and Cu–CoDAPyPTS–MCM-41-W synthesized by reaction of copper (II) nitrate using water as solvent are also studied in benzyl alcohol oxidation under solventless. In a typical run, 25 mmol of benzyl alcohol, 32 mmol of oxidant (TBHP or H<sub>2</sub>O<sub>2</sub>) and 0.25 g of copper catalyst, are stirred and heated (367 K, 4 h and 367 K, 30 min, respectively).

##### 3.4.1. Benzyl alcohol oxidation with TBHP

The results in the oxidation of benzyl alcohol over Cu–DAPyPTS–MCM-41-W and Cu–CoDAPyPTS–MCM-41-W catalysts and using TBHP as oxidant are shown in Table 3. As can be seen both catalysts exhibit conversion values comparable and, thus, independent on the parent hybrid material (DAPyPTS–MCM-41 and CoDAPyPTS–MCM-41) and on the copper loading. Unexpectedly, these materials, synthesized in aqueous media reveal better conversion (58% and 62%) to those prepared in organic media with lower copper contents. However, the decrease in selectivity is highly noticeable in the case of the use of Cu–DAPyPTS–MCM-41-W catalyst (32% selectivity) in comparison with Cu–DAPyPTS–MCM-41 catalyst (86% selectivity). For Cu–CoDAPyPTS–MCM-41-W and Cu–CoDAPyPTS–MCM-41 catalysts similar selectivities 42 and 46%, respectively, are obtained. According to TOF parameter (Table 3) Cu–DAPyPTS–MCM-41-W is the catalyst that presents the higher catalytic activity with 155 TOF value.

##### 3.4.2. Benzyl alcohol oxidation with H<sub>2</sub>O<sub>2</sub>

Several time periods have been studied before fixing the experimental conditions, 30 min, for the catalytic tests using hydrogen peroxide as oxidant. Higher times decrease enormously selectivity values towards benzaldehyde, increasing the amount of benzoic acid obtained as side product. The obtained results summarized in Table 4 shows that the use of H<sub>2</sub>O<sub>2</sub> as oxidant gives lower conversion values than those achieved with TBHP as previously have been observed. Again, the conversion results for the catalysts Cu–DAPyPTS–MCM-41-W and Cu–CoDAPyPTS–MCM-41-W are comparable and independent on the parent hybrid material and on the copper loading. In accordance with TOF parameter,

Cu–DAPyPTS–MCM-41-W is the catalyst that presents the higher catalytic activity with 420 TOF value and higher selectivity of 45%. Recently, TOF values have been reported by Bansal et al. [9] with tetraazamacrocyclic complexes of Cu(II) as catalysts are in the range 110–123 h<sup>-1</sup>.

In order to determine whether the active species leached into solution during a typical run, control filtrate experiments were performed. Two samples of the copper supported precursor Cu–DAPyPTS–MCM-41 was stirred during 30 min in the presence of TBHP and benzyl alcohol in 10/25/32 molar ratio. One of the mixtures was then filtered off and the filtrate was stirred 3.5 additional hours under similar experimental conditions, after the appropriate work up the filtrate shows a 5% conversion and 80% selectivity, meanwhile the second sample stirred 4 h shows 36% and 86% conversion and selectivity, respectively; indicating that leaching of catalytically active copper species into solution is negligible.

In representative tests, the catalysts Cu–DAPyPTS–MCM-41-W and Cu–CoDAPyPTS–MCM-41-W were filtered out after the experiment, dried in an oven at 160 °C for 6 h and reused twice. The obtained results (Table 4) show that these materials can be recovered and reused without significant loss of catalytic activity.

With regard to the reaction mechanism further studies are currently underway but according to literature [3] the results suggest the formation of a copper-peroxo and copper alcoholate intermediates by the coordination of alcohol to copper centres. The alcoholate species undergoes typical β-elimination to afford the corresponding carbonyl compound and the copper heterogenized complex, so the cycle can be repeated as suggests the re-used experiments. Using TBHP as oxidant the catalysts prepared in aqueous media, Cu–DAPyPTS–MCM-41-W and Cu–CoDAPyPTS–MCM-41-W, revealed higher efficiency in the oxidation of benzyl alcohol to benzaldehyde than those prepared in organic media Cu–DAPyPTS–MCM-41 and Cu–CoDAPyPTS–MCM-41, this fact may be due to the easier coordination of peroxide and alcohol substrate to the acucopper complexes, covering the silica surface, by water replacement in the former materials than the replacement of nitrate ligand in the latter ones. In presence of hydrogen peroxide the active catalyst must derive from ionized species capable of anchoring peroxide units in both types of materials, giving conversion values much more dependent on the copper content [35].

## 4. Conclusions

Copper-containing catalysts have been synthesized by immobilization of copper (II) ethylacetoacetate or copper (II) nitrate precursors onto previously organofunctionalized MCM-41 materials with *N*<sup>4</sup>-(3-(triethoxysilyl)propyl)pyrimidine-2,4,6-triamine (DAPyPTS) compound. Comparison between the Cu anchoring efficiency of both precursors shows that the materials synthesized by immobilization of copper (II) ethylacetoacetate present high anchored efficiency, providing complexes with nearly 1:2 stoichiometry. CuAc–DAPyPTS–MCM-41 catalyst shows highest selectivity to benzaldehyde (97%) for solvent-free oxidation of benzyl alcohol using TBHP as oxidant. The catalysts prepared in aqueous medium, Cu–DAPyPTS–MCM-41-W and Cu–CoDAPyPTS–MCM-41-W, exhibit better conversion results (62 and 58%, respectively) than those obtained with the catalysts synthesized in organic medium, Cu–DAPyPTS–MCM-41 (36% conversion) and Cu–CoDAPyPTS–MCM-41 (54% conversion). However, in the case of Cu–DAPyPTS–MCM-41-W catalyst a decrease in selectivity is highly noticeable in comparison with Cu–DAPyPTS–MCM-41 catalyst (32 and 86%, respectively). When H<sub>2</sub>O<sub>2</sub> is used as the oxidant, 39% conversion is obtained in 30 min

using Cu–DAPyPTS–MCM-41 as catalyst. Nevertheless, with H<sub>2</sub>O<sub>2</sub> as oxidant the selectivity to benzaldehyde is relatively lower than it is achieved using TBHP as oxidant.

### Acknowledgement

We gratefully acknowledge financial support from the MICINN (project CTQ2008-05892/BQU).

### References

- [1] V.R. Choudhary, D.K. Dumbre, V.S. Narkhede, S.K. Jana, Catal. Lett. 86 (2003) 229–233.
- [2] S. Ajaikumar, A. Pandurangan, J. Mol. Catal. A: Chem. 290 (2008) 35–43.
- [3] A. Puzari, J.B. Baruah, J. Mol. Catal. A: Chem. 187 (2002) 149–162.
- [4] K.O. Xavier, J. Chaco, K.K. Mohammed Yusuff, Appl. Catal. A: Gen. 258 (2004) 251–259.
- [5] C.N. Kato, M. Hasegawa, T. Sato, A. Yoshizawa, T. Inoue, W. Mori, J. Catal. 230 (2005) 226–236.
- [6] V.R. Choudhary, D.K. Dumbre, B.S. Uphade, V.S. Narkhede, J. Molec. Catal. A: Chem. 215 (2004) 129–135.
- [7] V.B. Valodkar, G.L. Tembe, M. Ravindranathan, R.N. Ram, H.S. Rama, J. Mol. Catal. A: Chem. 208 (2004) 21–32.
- [8] V.R. Choudhary, P.A. Chaudhari, V.S. Narkhede, Catal. Commun. 4 (2003) 171–175.
- [9] V.K. Bansal, P.P. Thankachana, R. Prasad, Appl. Catal. A: Gen. 381 (2010) 8–17.
- [10] A. Abad, C. Almela, A. Corma, H. Garcia, Chem. Commun. (2006) 3178–3180.
- [11] (a) K. Mori, T. Hara, T. Mizugaki, K. Ebitani, K. Kaneda, J. Am. Chem. Soc. 126 (2004) 10657–10666;  
(b) B. Karimi, S. Abedi, J.H. Clark, V. Budarin, Angew. Chem. Int. Ed. 45 (45) (2006) 4776–4779.
- [12] (a) Y. Chen, H. Lim, Q. Tang, Y. Gao, T. Sun, Q. Yan, Y. Yang, Appl. Catal. A: Gen. 380 (2010) 55–65;  
(b) P.J. Miedziak, Q. Heb, J.K. Edwardsa, S.H. Tylora, D.W. Knighta, B. Tarbitc, C.J. Kielyb, G.J. Hutchings, Catal. Today 163 (2011) 47–54.
- [13] A. Hamza, D. Srinivas, Catal. Lett. 128 (2009) 434–442.
- [14] X. Wang, G. Wu, J. Li, N. Zhao, W. Wei, Y. Sun, J. Mol. Catal. A: Chem. 276 (2007) 86–94.
- [15] M.J. Alcón, A. Corma, M. Iglesias, F. Sánchez, J. Mol. Catal. A: Chem. 194 (2003) 137–152.
- [16] P. Karandikar, K.C. Dhanya, S. Deshpande, A.J. Chandwadkar, S. Sivasanker, M. Agashe, Catal. Commun. 5 (2004) 69–74.
- [17] A. Sakthivel, W. Sun, G. Raudaschl-Sieber, A.S.T. Chiang, M. Hanzlik, F.E. Kühn, Catal. Commun. 7 (2006) 302–307.
- [18] W.A. Carvalho, M. Wallau, U. Schuchardt, J. Mol. Catal. A: Chem. 144 (1999) 91–99.
- [19] T. Tsoncheva, Tz. Dimitrov, C. Minchev, K. Hadjiivanov, J. Mol. Catal. A: Chem. 209 (2004) 125–134.
- [20] S. Jana, S. Bhunia, B. Dutta, S. Koner, Appl. Catal. A: Gen. 392 (2011) 225–232.
- [21] R. Ballesteros, D. Pérez-Quintanilla, M. Fajardo, I. Hierro, I. Sierra, J. Porous Mater. 17 (2010) 417–424.
- [22] Y. Li, B. Yang, J. Solid State Chem. 181 (2008) 1032–1039.
- [23] N.L. Dias Filho, Colloids Surf. A Physicochem. Eng. Aspects 144 (1998) 219–227.
- [24] O. Olfovyyk, M. Jaroniec, Adsorption 11 (2005) 205–214.
- [25] T. Yokoi, H. Yoshitake, T. Tatsumi, J. Mater. Chem. 14 (2004) 951–957.
- [26] S. Udayakumar, Y.-S. Son, M.-K. Lee, S.-W. Park, D.-W. Park, Appl. Catal. A: Gen. 347 (2008) 192–199.
- [27] R. Deters, R. Krämer, Inorg. Chim. Acta 269 (1998) 117–124.
- [28] A.R. Silva, K. Wilson, A.C. Whitwood, J.H. Clark, C. Freire, Eur. J. Inorg. Chem. (2006) 1275–1283.
- [29] A.M. Klonkowski, B. Grobelna, T. Widernik, A. Jankowska-Frydel, W. Mozgawa, Langmuir 15 (1999) 5814–5819.
- [30] M. Gaye, O.-. Sarr, A.S. Sall, O. Diouf, S. Hadabere, Bull. Chem. Soc. Ethiop. 11 (1997) 11–119.
- [31] M. Salavati-Niasari, S. Abdolmohammadi, J. Porous Mater. 16 (2009) 19–26.
- [32] M.H. Lim, A. Stein, Chem. Mater. 11 (1999) 3285–3295.
- [33] Q. Yanga, M.P. Kapoora, S. Inagakia, N. Shirokurac, J.N. Kondoc, K. Domen, J. Mol. Catal. A: Chem. 230 (2005) 85–89.
- [34] I.K. Mbaraka, B.H. Shanks, J. Catal. 229 (2005) 365–373.
- [35] S. Sharma, N. Barooah, J.B. Baruah, J. Mol. Catal. A: Chem. 229 (2005) 171–176.
- [36] A.J. Blake, M.T. Brett, N.R. Champness, Chem. Commun. (2001) 2258–2259.
- [37] B.J. Holliday, C.A. Mirkin, Angew. Chem. Int. Ed. 40 (2001) 2022–2043.
- [38] Q. Yang, M.P. Kapoora, S. Inagakia, N. Shirokurac, J.N. Kondoc, K. Domen, J. Mol. Catal. A: Chem. 230 (2005) 85–89.